Pressure dependence of the measured line intensity and super-Lorentzian effects in the absorption spectra of pure HCl

Ha Tran, Gang Li, Ngoc Hoa Ngo, Volker Ebert

Pressure dependence of the measured line intensity and super-Lorentzian effects in the absorption spectra of pure HCl

Ha Tran, *[a] Gang Li,[b] Ngoc Hoa Ngo,[c] Volker Ebert,[b,d]

Abstract: Super-Lorentzian effects in the troughs between lines and the pressure dependence of the line intensities retrieved from fits of absorption spectra of pure HCl have been investigated both experimentally and theoretically. For that, spectra of pure HCl gas in the 2-0 band were recorded with a Fourier Transform spectrometer at room temperature and for pressures ranging from 1 to 10 atm. The line intensities, retrieved from fits of the measurements with the Voigt profile using a single spectrum fitting technique, reveal large decreases with increasing pressure - up to 3% per atm - with a relatively weak rotational dependence. We also show that the absorptions in between successive P and R transitions are significantly larger than those predicted using Voigt profiles. Requantized classical molecular dynamics simulations were made in order to predict absorption spectra of pure HCl matching the experimental conditions. The pressure dependence of the intensities retrieved from the calculated spectra as well as the predicted super-Lorentzian behavior between lines are in good agreement with the measurements. Our analysis shows that these effects are essentially due to incomplete collisions, which govern the dipole auto-correlation function at very short times.

1. Introduction

Super-Lorentzian effects in the troughs between lines have been observed a long time ago in the absorption spectra of pure HCl[1], HCl diluted in CO_2,[2,3] and more recently for HCl in Ar[4]. This manifests through the fact that the measured absorption in the troughs between transitions exceeds that predicted using the Lorentzian profile. Furthermore, it was also shown that, for lines of small rotational quantum number, the line intensities (or the integrated line shapes) retrieved from fits of measured spectra with the Lorentzian line shape decrease linearly with the perturber pressure (see Ref. [5] for HF in Xe, Ref. [6] for HCl in Ar, and Ref. [7] for Xe-broadened HI lines). These effects were attributed to the non-Markovian behavior of collisions or the breakdown of the impact theory[4,6,8] and/or to the formation of gaseous molecular complexes[5,6,9]. From spectra of HCl diluted in Ar, measured between 10 and 50 atm, Boulet et al.[6] observed that this pressure dependence of the retrieved intensities quickly reduces with increasing rotational quantum number [e.g. for the P(1) line in the fundamental band, the intensity decrease is 0.78% per atm while for the P(3) line, it is 0.06% per atm only]. Using the model proposed in Ref. [5], they estimated the influence of the HCl-Ar complexes formation on the intensities of the monomer transitions. It was shown that the contribution of complex formation is about 6 times smaller than the observed intensity depletion. In Ref. [9], Vigasin et al attributed this effect to the formation of both true and quasi-bound complexes. They modified the model of Ref. [5] and deduced a damping amount due to the contribution of quasi-complexes formation. The obtained values are two to three times smaller than the observed decrease of the monomer line intensities (e.g. for HCl in Ar, they obtained 0.3% atm^{-1} for the J=0 line while experimental values range from 0.62 to 0.86% atm^{-1}). Then, the authors added an empirical contribution of true complexes in order to get a better agreement with observed values. In contrast, in Ref. [8], the intensity depletion observed for HCl in Ar and HF in Xe was attributed to the breakdown of the impact theory and not to the formation of complexes. In Tran et al.[4], using requantized classical molecular dynamics simulations (rCMDS), absorption spectra of HCl broadened by Ar in the 1-0 and 2-0 bands were computed. It was shown that super-Lorentzian effects in the troughs between lines of small rotational quantum number determined from the simulated spectra are in very good agreement with those obtained from experimental spectra. Analysis of the time evolution of the molecular populations for different rotational levels, computed by rCMDS, clearly showed that the super-Lorentzian behavior is essentially due to non-Markovian collisions.

Not limited to halide gaseous molecular systems, the pressure dependence of the experimentally determined line intensities has been recently observed for the first time for CO diluted in N_2[10]. Indeed, thanks to extremely precise and accurate measurements, it was demonstrated that the CO integrated line shape obtained by fitting a standard profile to spectra in the core region of an absorption line decreases with the gas density. At atmospheric pressure, this effect reduces the retrieved line intensity by about 0.3% for the first few rotational lines of CO diluted in N_2. These findings were also well supported by molecular dynamics simulations which enabled their attribution to the breakdown of the impact approximation and showed that the collisions ongoing at time zero transfer a fraction of the intensity from the core region of the line to a broad and weak continuum, and thus reduce its area.

In this study, super-Lorentzian effects in the troughs between lines and the pressure dependence of the experimentally determined line intensities are investigated in the absorption spectra of pure HCl which have been measured with a Fourier

[a] *Laboratoire de Météorologie Dynamique, IPSL, CNRS, Sorbonne Université, Ecole polytechnique, Institut polytechnique de Paris, École normale supérieure, PSL Research University, F-75005 Paris, France.*
[b] *Physikalisch-Technische Bundesanstalt, Bundesallee 100, 38116 Braunschweig, Germany.*
[c] *Faculty of Physics, Hanoi National University of Education, 136 Xuan Thuy, Cau Giay, Hanoi, Vietnam.*
[d] *Physikalisch-Chemisches Institut, Heidelberg University, INF 253, 69116 Heidelberg*
† corresponding author: ha.tran@lmd.jussieu.fr

Transform spectrometer (at 0.075 cm^{-1} resolution) for a wide pressure range, from 1 to 10 atm. rCMDS are carried out in order to compute the time evolution of the dipole auto-correlation function and derive the absorption spectra. The magnitudes of super-Lorentzian effects and of the intensity depletion predicted by the rCMDS are then compared with experimental results. The paper is organized as follows: Section 2 is devoted to the description of the measurements and of the analysis procedure. The rCMDS are detailed in Sec. 3, while comparisons between experimental results and theoretical predictions are presented and discussed in Sec. 4. Conclusions are drawn in Sec.5.

2. Experiment and analysis

2.1 Experimental setup and conditions

The experimental setup has been described in detail previously for related measurements of pure HCl[11], HCl mixed with CO/CO_2[12], and HCl mixed with H_2/CH_4[13]. In brief, HCl gas was generated in a glass generator by the reaction of sulfuric acid (H_2SO_4) with sodium chloride (NaCl). HCl gas was then condensed in a liquid nitrogen (LN_2) cooled trap until enough solid HCl was formed. The generation and storage equipment were kept in a venting chemical fume hood together with a 5.34±0.1 cm long aluminum gas cell for spectroscopic measurements. The absorption cell, gas manifolds, and the LN_2 trap were evacuated for 10 minutes to remove water vapor and semi-volatile compounds stuck on the walls. Prior to the FTIR measurements, the liquid nitrogen trap was heated up and the vaporized HCl gas (at up to 13.3 bar) was directed into the measurement cell. For consecutive FTIR measurements, the cell pressure was progressively reduced stepwise with steps of 0.5 to 1 bar. Table 1 summarizes the sampling conditions.

Sample	Initial pressure (bar)	End pressure (bar)	Pressure step (bar)	Temperature (°C)	Temperature stability (°C)
Pure HCl	13.3	1.0	0.5/0.1	20.05	0.05

Table 1: Sampling conditions of the FTIR measurements of pure HCl. The stability of temperature is accounted for the period of one spectrum consisting of 10 scans.

To avoid fringes in the FTIR spectra, the gas cell was sealed on both sides with wedged (1°) sapphire windows with 1" diameter. The aluminum cell has a natural Al_2O_3 layer which is inert to HCl at room temperature. To record the FTIR spectra, the recombined light after the KBr beam splitter of the FTIR spectrometer (*Bruker Optics, Vertex 80*) was coupled into a fume hood through a multi-mode optical fiber, then collected with a spherical mirror to form a free-space light-beam, which was directed through the gas cell and onto a standalone near infrared (NIR) InGaAs detector. The digitized signal of the detector was sent back to the spectrometer's electronic board to record the interferogram. *OPUS* FTIR software by Bruker Optics was used to control the spectrometer for scanning and data recording.

The pressure in the gas cell was monitored with a piezoresistive pressure transmitter (*Omega® PAA33X-V-30,* 0 - 3 MPa, 0.15% rel. accuracy according to the manufacturer calibration). The relative pressure stability inside the cell was found to be 0.02%. Based on previous experience, we estimated a 0.3 % combined, relative expanded uncertainty (k=2, 95% confidence level) of our pressure measurement also accounting for zero-drifting over time. The lab temperature was regulated with a central air conditioning unit to 20±0.5 degrees Celsius. The body temperature of the gas cell was monitored with a Type-K thermocouple attached to the outside. Within the recording time for one spectrum (of about 100 seconds) the cell temperature was stable within +/-0.05 °C. The path length of the gas cell was determined by subtracting the thickness of the sapphire windows from the total cell length measured with a caliper. We estimated the total uncertainty of our length measurement to be 1 mm (k=2, 95% confidence level).

Table 2 summarizes the FT spectrometer (FTS) configuration for our measurements. Basically, the Vertex 80 FTS was equipped with a Globar source, a KBr beam splitter and a remotely connected InGaAs NIR detector inside the fume hood. For each pressure step of 0.5 bar, ten interferograms were recorded and coadded at a spectral resolution of 0.075 cm^{-1} (defined as 0.9/MOPD, where MOPD denotes the maximum optical path difference of the FTS). The Fourier transform algorithm built in the OPUS software was applied to the measured interferograms to derive the sample signal (I_{sample}), i.e. the intensity spectrum after transmission through the gas cell. Transmittance spectra were calculated by dividing I_{sample} with the background signal ($I_{background}$) which was measured with the empty cell before the HCl addition, i.e. $T = I_{sample}/I_{background}$. A boxcar apodization function and a *Mertz* phase correction were applied during the finite Fourier transform algorithm.

Measurement parameter	
Detector	InGaAs
Beam Splitter	KBr
Spectral resolution	0.075 cm^{-1}
Record time	100s each spectrum (10 scans)
Aperture diameter	0.5 mm
Apodization function	Boxcar
Phase correction	Mertz
Gas cell length	5.34±0.1 cm
Gas cell windows	Sapphire (1° wedge, 1" diameter)
Gas Pressure	Piezo resistive gauge up to 3MPa
Gas temperature	Type K Thermocouple

Table 2: Configuration of the Bruker Optics Vertex 80 FTIR spectrometer and the HCl gas cell.

2.2 ILS determination

The Instrumental line shape (ILS) function of the FTS was determined by applying the LINEFIT14.5 software[14,15] on a measured, low-pressure (0.05 atm) spectrum of pure HCl. Figure 1 shows the retrieved instrumental parameters, namely the modulation efficiency and the phase error versus the different optical path differences.

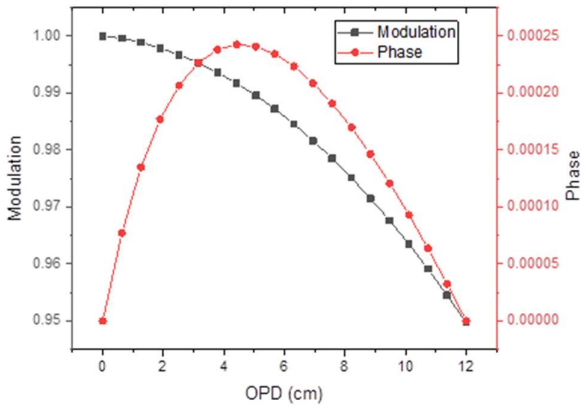

Figure 1: Retrieved FTS instrumental line shape (ILS) parameters using the LINEFIT14.5 software.

2.3 FTS spectral analysis procedure

We first used the spectroscopic parameters previously obtained from fits of pure HCl spectra measured at pressures lower than 1.2 atm[11] to compute absorption spectra, over the entire band, under the exact experimental conditions considered in this work. Figure 2 shows the ratio between the measured absorption coefficient, α_{exp}, and the calculated one, α_{Voigt}, for some pressures. These examples demonstrate a strong super-Lorentzian behavior between the lines within the central region of the band, since $\alpha_{exp}/\alpha_{Voigt}$ is well above unity, similar to the observations for HCl-CO_2[2] and HCl-Ar mixtures[4].

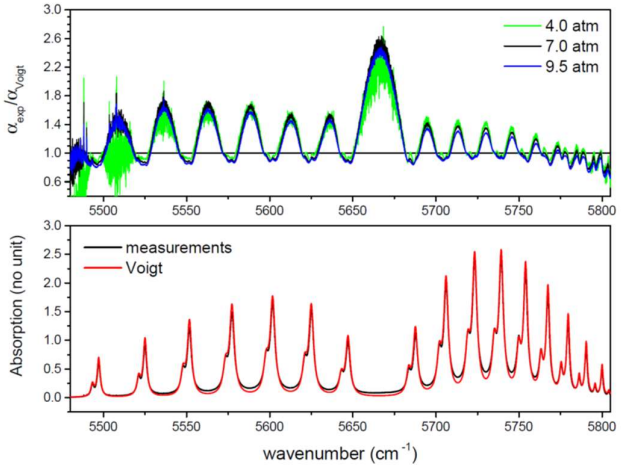

Fig. 2: *Bottom:* Measured absorptions and corresponding Voigt calculations in the 2-0 band of pure HCl at 7 atm. *Top:* Ratio between measured and calculated spectra for P = 4, 7 and 9.5 atm.

While the Voigt line-shape calculations underestimate the absorption in the troughs between lines, they predict values lower than the measured ones at the line centers with $\alpha_{exp}/\alpha_{Voigt}$ well below unity. This behavior is different from what was observed for HCl in Ar[4] where $\alpha_{exp}/\alpha_{Voigt}$ is very close to 1 at line centers. Figure 2 also shows that the absorption becomes sub-Lorentzian when going away from the center toward the band wings.

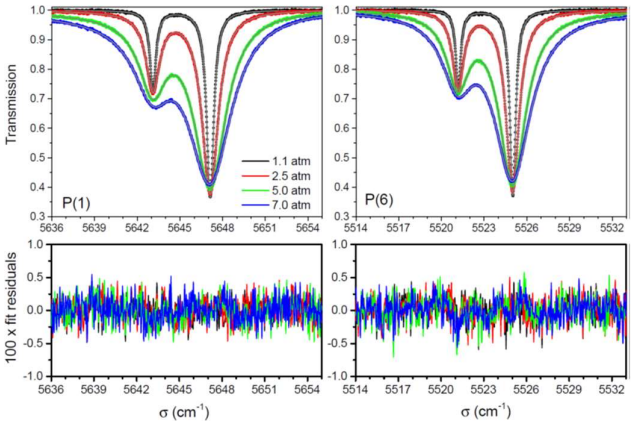

Fig. 3: Spectra of the $P(1)$ (left) and $P(6)$ (right) lines of self-broadened HCl measured (dots) at room temperature, for various pressures and their fits (full line) using the Voigt profile with first-order line-mixing. The corresponding fit residuals are displayed in the bottom panel.

In the second step, we fitted each line of each measured spectrum considered here, with the usual Voigt model. Line-mixing was taken into account using the first-order approximation[16]. The calculated spectrum was convolved with the ILS described above. A spectral range of about 20 cm^{-1} including two transitions of the same rotational quantum number of two isotopologues $H^{35}Cl$ and $H^{37}Cl$ was considered for each fit. The position (including the pressure-induced line shift), Lorentzian width, first-order line-mixing parameter, and the area of the $H^{35}Cl$ line were adjusted. For the $H^{37}Cl$ line, its difference in frequency with the corresponding $H^{35}Cl$ line and their intensity ratio were fixed to values provided in HITRAN[17] while their line widths (as for line mixing) were assumed to be the same. The Doppler half-widths were fixed to the theoretical values computed for each line using the measured cell temperature. In order to test the influence of the baseline on the retrievals, each fit was performed with two baseline functions: A linear and a cubic baseline whose parameters were also adjusted. Figure 3 displays some examples of the obtained fits and residuals, showing very good agreements between the measured and adjusted spectra. As can be observed, the spectral residuals are within the experimental noise, and there is therefore no need for the use of more refined line-shape models. Note that tests have been performed in which the measured spectra of the P(1) line were fitted with the Nelkin-Ghatak and the quadratic speed dependent Voigt profiles showing fits residuals which are very similar to those obtained with the Voigt profile.

The self-broadening coefficients were then obtained from linear fits of the retrieved line widths versus pressure (Fig. 4a). Since the HCl gas shows large deviations from the ideal gas law for the considered pressures, we introduced the *"equivalent"* pressure: From the measured gas temperature and gas pressure, we first computed the HCl gas density taking into account the second virial coefficient[18]. From this density, the "ideal gas" equivalent pressure is then deduced. Note that for a better determination of the line broadening, only the values obtained at equivalent pressures lower than 6 atm were retained. The obtained values are plotted in Fig. 4b and compared with the measured values of Ref. [11] as well as those provided in the HITRAN database[17]. In Ref. [11], data were deduced from fits of spectra measured for the 2-0 band, at pressures lower than 1.2 atm while those in the HITRAN database were obtained by scaling values in the fundamental band which were obtained from spectra measured at pressures lower than 0.26 atm[19,20]. A good general agreement is observed with an average relative difference of 0.6 (± 4.2) % and 2.3 (± 1.3) % when comparing our values with those of Ref. [17] and Ref. [11], respectively.

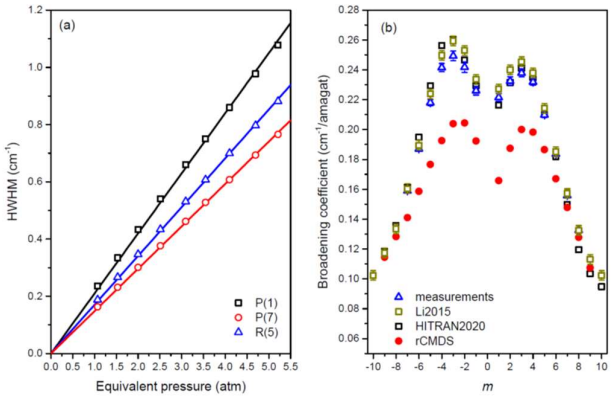

Fig. 4: (a) Examples of the measured half-width at half-maximum (HWHM) in the 2-0 band of pure HCl and linear fits vs the equivalent pressure. (b) Comparisons between the line broadening coefficients obtained in this work (blue triangles, see sec. 2.3) and measured values of Ref. [11] (dark yellow squares) as well as those provided in HITRAN2020 (black squares)[17] for the 2-0 band of H^{35}Cl. Those deduced from the rCMDS-calculated spectra (red circles, see Sec. 3) are also displayed. m refers to the rotational quantum number, $m = -J$ for P and $m = J + 1$ for R branch lines.

In Fig. 5a are plotted examples for the retrieved line area, A_{exp}, versus the equivalent pressure (which is from now on called "pressure" for simplicity) for the $P(1)$ and $P(4)$ lines. This clearly shows that these values are not linear with the HCl pressure (or the HCl number density), while it should be the case if the retrieved line area was directly the product of the line intensity with the active molecule pressure (or density) as widely assumed. The pressure-normalized line area, which will be called the "*retrieved line intensity*", $S_{exp} = A_{exp}/P$, obtained for various $P(J)$ lines, is displayed in Fig. 5b. For clarity, S_{exp} is here normalized to its corresponding value at zero pressure, S_0, which was determined as the intercept, at $P = 0$, of the linear fit of S_{exp} versus pressure [i.e. $S_{exp} = S_0(1 - P \times \Delta S_{exp})$]. The slope of this linear fit provides an intensity correction parameter, ΔS_{exp}, which characterizes the linear pressure dependence of the retrieved line intensity. For the $P(1)$ and $P(7)$ lines for instance, ΔS_{exp} is 3.22 (± 0.07) and 2.56 (± 0.06) %/atm. The results obtained for all considered lines are presented and discussed in Sec. 4.

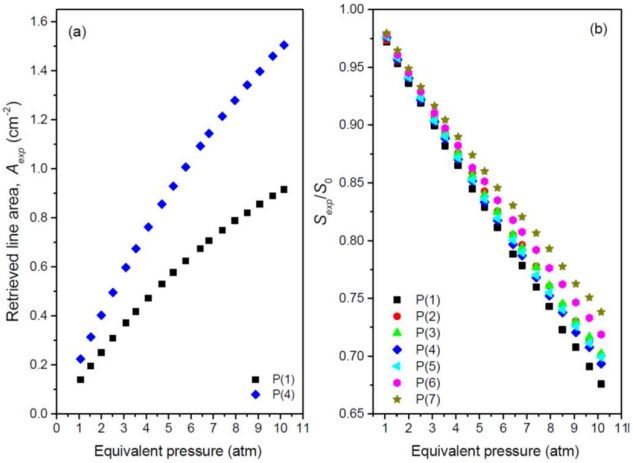

Fig. 5: (a) The line areas A_{exp}, retrieved from fits of measured spectra with the Voigt profile and first-order line-mixing for the $P(1)$ and $P(4)$ lines vs the equivalent pressure. (b) Ratio of the measured intensity, S_{exp}, to value at zero pressure S_0 (determined as the interception of the linear fit of the retrieved intensity vs pressure).

3. Requantized classical molecular dynamics simulations

Classical molecular dynamics simulations (CMDS) were performed for pure HCl using the procedure detailed in Refs. [4,21] and based on the equations given in Ref. [22]. We considered a large number of molecules placed in several cubic boxes with periodic boundary conditions. Each molecule, considered as a rigid rotor, is characterized by its center-of-mass position and velocity, by a unit vector along the molecular axis and by its angular velocity vector. At the initial time, the center-of-mass position, the orientations of the translational and angular velocities as well as the molecular axis direction were randomly chosen. Maxwell-Boltzmann distributions were applied to the initial values of the modulus of the translational and angular velocities. The molecules positions were chosen such that they should be at least 7 Å away from each other to avoid unphysical situations associated with too close pairs. This condition will require a thermalization time which is the time necessary for the system to come to equilibrium. Based on an input intermolecular potential and the initial conditions, the time evolutions of the above-mentioned molecular parameters are computed using classical mechanics, as done in Ref. [21]. Specifically, we computed the position of each molecule at time t. Then, if there is another molecule close enough to the current one (when the distance between two molecules is less than a cut-off distance for the interaction to be significant), we compute the total force (and torque) applied to the former. This enables us to determine the acceleration of the center-of-mass and to change its translational velocity which is then used to compute of the new position of the particle at time $t + dt$. The

angular velocity and the molecular orientation are also incremented from t to $t + dt$. The requantization procedure described in Refs. [4,21] was used here for the rotation of the HCl molecules. The auto-correlation function (ACF) of the dipole moment, carried by the molecular axis, was computed for each time step. Its Fourier-Laplace transform directly yields the corresponding absorption spectrum. Such calculations were previously made for HCl in Ar showing that the deduced line broadening coefficients, line profiles as well as super-Lorentzian effects in the troughs between lines are in good agreement with measured values[21].

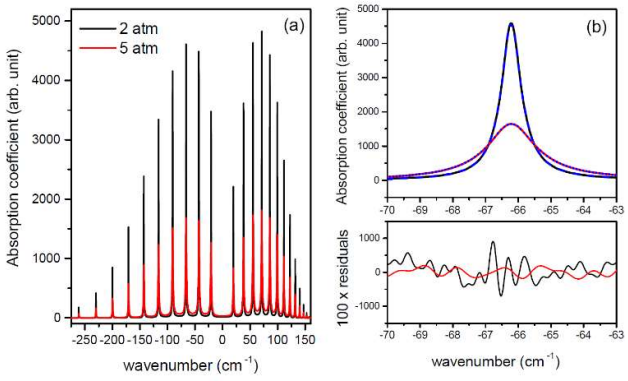

Fig. 6: (a) Spectra of the 2-0 band of pure HCl, obtained from the Fourier-Laplace transform of the ACFs of the dipole moment computed by rCMDS at room temperature and for pressure of 2 (black) and 5 (red) atm. (b) In the top panel are spectra of the P(3) line, computed at 2 (black) and 5 (red) atm and their corresponding Lorentzian fits (blue dots) while the fit residuals are plotted in the bottom panel.

Requantized CMDS (rCMDS) were made for pure HCl at 296 K and 1, 2, 3 and 5 atm. The bond length of the HCl molecule was set to 1.275 Å and only $H^{35}Cl$ was considered. The HCl-HCl interaction is represented by the site-site pair potential provided by Ref. [18]. It is a modified Morse potential complemented by Coulombic interactions whose parameters were obtained from fits of an ab initio intermolecular potential. The calculations were performed from $-t_{tempo}$ (t_{tempo} is the duration needed for the system to reach thermodynamic equilibrium) to t_{max} with a time step of 0.8 fs. t_{max} varied from 50 to 200 ps depending on the pressure considered, with smaller t_{max} being needed for the ACF to be converged at higher pressure. The Fourier-Laplace transform of the ACF, calculated from $t = 0$ to t_{max} directly provides the absorption spectrum of HCl[21]. Examples of obtained spectra are presented in Fig. 6a.

The rCMDS-calculated spectra were then fitted with the Lorentz line-shape model, with first-order line mixing accounted for, exactly as what was done for the measurements, two examples of fit residuals being presented in Fig. 6b. Since the Doppler effect was omitted in the calculations, the Lorentz model was used instead of the Voigt profile. The impact of the limited value of t_{max}, leading to truncated ACFs, was taken into account by convolving the calculated spectrum with a sinus cardinal function of argument $2\pi c\sigma t_{max}$. The obtained line broadening coefficients and line intensities are presented and compared with experimental values in Sec. 4.

4. Results and discussions

The line broadening coefficients determined from linear adjustments of the collisional line widths retrieved from the rCMDS-calculated spectra versus pressure, are plotted together with measured values in Fig. 4b, which shows that the predicted values are from 6 to 20% smaller than the measured ones. This can be explained, at least partially, by the classical treatment of molecules with relatively large rotational constants such as HCl. Furthermore, rCMDS do not take into account the vibrational dependence of the potential and its effect on the line broadenings[6]. The pressure dependences of the line intensities, S_{rCMDS}, deduced from simulations are exemplified in Fig. 7 where a linear decrease, consistent with the experimental findings (Fig. 5b), is clearly observed.

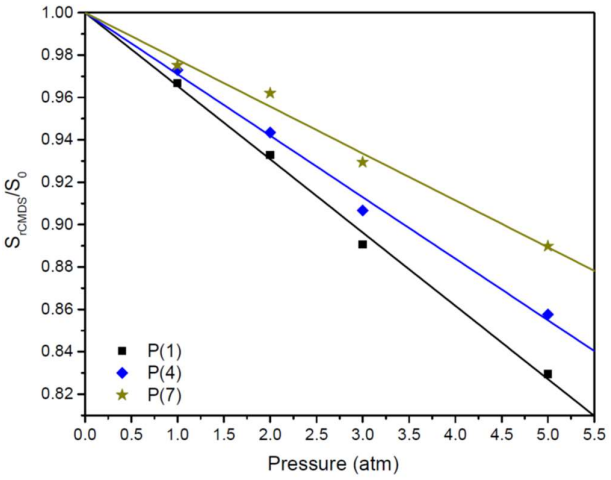

Fig. 7: The pressure dependence of the line intensity, S_{rCMDS}, retrieved from the rCMDS-calculated spectra. S_{rCMDS} was here normalized to value at zero pressure, as what was done for the measurements (Fig. 5b).

The slopes obtained from linear fits of S_{rCMDS}/S_0 directly yield the predicted intensity correction parameters, ΔS_{rCMDS}. The latter are displayed in Figure 8 together with the values deduced from experimental spectra. The reported uncertainties take into account the standard deviations obtained from the linear fits. In addition, as mentioned in Sec. 2.3, we varied the baseline function (linear or cubic vs wavenumber) for each line fitting of the measured (or calculated) spectrum. This led to slightly different retrieved intensities and their pressure dependence, which were also accounted for in the reported uncertainties. As can be observed in Fig. 8, the rCMDS results are in relatively good agreement with measured values, both showing large intensity corrections, which slowly decrease with

increasing rotational quantum number. The effect is thus here much larger than that observed for HCl in Ar (weaker than 1% per atm)[6] and HF in Xe (smaller than 2% per atm)[5]. Furthermore, in these previous studies, it was shown that the effect is significant only for the first rotational quantum numbers (i.e. for $|m| \leq 2$) and becomes almost negligible for higher values of $|m|$ (e.g. $\Delta S \approx 1.8$ and 0.2 %/atm for the 1-0 R(1) and R(3) lines of HF in Xe[5] and $\Delta S = 0.86$ and 0.15 %/atm for the 2-0 R(1) and R(3) lines of HCl in Ar[6]). This is, as discussed later, probably due to the strong and long-range dipole-dipole interaction of pure HCl.

Fig. 8: The intensity correction parameters determined from measured spectra and comparison with that deduced from the rCMDS-computed spectra.

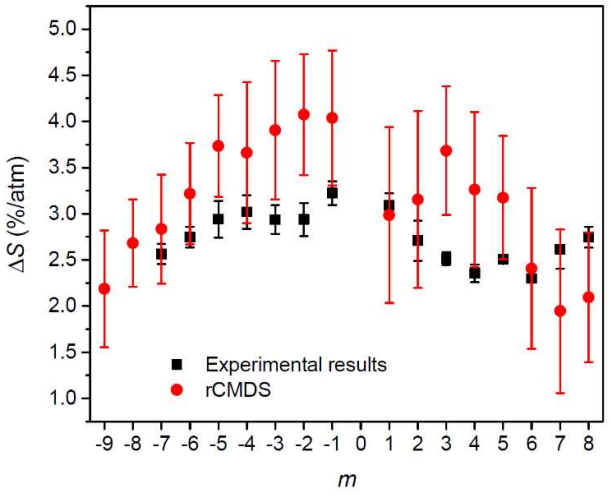

The positions, line intensities at zero pressure, and the line-shape parameters retrieved from the rCMDS spectra as described before were then used to simulate a spectrum at 5 atm using the Lorentzian profile. Figure 9 displays the ratio between this spectrum and that directly computed from rCMDS at the same pressure, $\alpha_{rCMDS}/\alpha_{Lorentz}$. The values of $\alpha_{exp}/\alpha_{Lorentz}$, obtained for the spectrum measured at 5 atm are also plotted for comparison.

Overall, the rCMDS do well reproduce the magnitude of the observed super-Lorentzian behavior in the troughs between lines as well as its rotational dependence. At the line centers, both experimental and predicted values are smaller than unity due to the intensity depletion effect. The fact that the theoretical values of $\alpha/\alpha_{Lorentz}$ in the troughs between lines, characterizing the super-Lorentzian effects, are larger than the measured ones is somehow consistent with the results obtained for the intensity correction parameter (Fig. 8) where ΔS_{rCMDS} is also larger than ΔS_{exp}. This could be due to the accuracy of the intermolecular potential used as well as to the classical treatment of the present method. Note that the only input needed for our rCMDS is the intermolecular potential, which is here a site-site functional form adjusted to an ab initio potential, taken from a completely independent study[18]. With no adjusted nor empirical parameters, the agreements observed for the pressure dependence of the retrieved line intensity and for the super-Lorentzian effects on the line shape demonstrate the quality of the theoretical predictions.

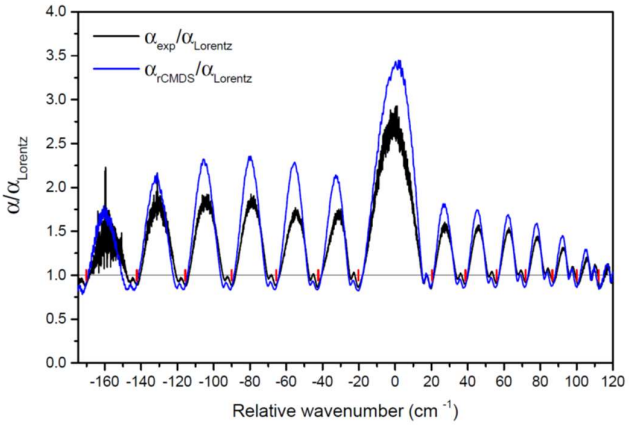

Fig. 9: Comparison between the ratios, $\alpha_{rCMDS}/\alpha_{Lorentz}$, obtained from the rCMDS-calculated spectra (blue) and those determined from experiments, $\alpha_{exp}/\alpha_{Lorentz}$ (black) for pure HCl in the 2-0 band at room temperature and 5 atm. In red are the unperturbed relative positions of the $H^{35}Cl$ lines.

To qualitatively explain these results, similarly to what was done for CO[10], we computed the time evolution of the relative number of molecules which are at the rotational quantum level J at time zero and remain at this level at time t, $\rho_J(t)/\rho_J(t = 0)$. If we neglect the influence of line mixing and the contribution of dephasing collisions to the decay of the dipole auto-correlation function, the spectrum of the line J is directly obtained from the Fourier transform of $\rho_J(t)$[4,23]. The results exemplified in Fig. 10a,b show that for times larger than about 0.5-1 ps, the population clearly follows an exponential decay while, for earlier times, it decreases significantly faster (see Fig. 10b).

As explained in Refs. [4,10], this non-Markovian behavior is due to the contribution of collisions that are ongoing at time zero. Indeed, for a given HCl-HCl relative orientation, the HCl-HCl potential V(R) with R the intermolecular distance, presents a repulsive front [where V(R) is 500 K for instance] for distances R_{min} of about 3 Å and its attractive part vanishes [where V (R) is -20 K for instance] for R_{max} of about 6.5 Å. The relative number of molecules experiencing a collision at $t = 0$ corresponds to those having a partner between the two spheres of radii R_{min} and R_{max}. For HCl at atmospheric density conditions corresponding to 296 K and 101.3 kPa, this number is ≃0.0257 which is of the same order of magnitude as the intensity correction factor ΔS (Fig. 8).

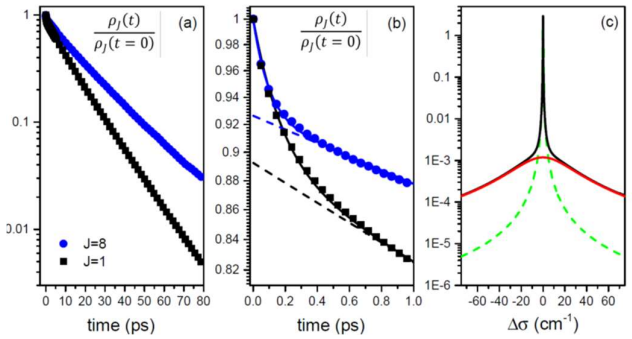

Fig. 10: (a) and (b): Normalized populations for pure HCl at 2 atm and 296 K for two rotational quantum numbers $J = 1$ and $J = 8$ at different time scales. The rCMDS results are in symbols while the lines are their fits using Eq. (1) (solid lines) and using a single exponential decay function for times larger than 1 ps (dash lines). (c) Line spectrum for $J = 1$ (black) calculated as the Fourier-Laplace transform of the relative population associated with the long- (green) and short-time (red) exponential decays of the populations.

In order to go further, the relative populations, computed at various pressures *P*, were fitted with the following function:

$$\rho_J(t)/\rho_J(t=0) = (1 - Pa_J)e^{-P\,/\tau_J^\infty} + Pa_J e^{-t/\tau_J^0}, \qquad (1)$$

in which the first term is related to the long-time scale evolution of $\rho_J(t)/\rho_J(t=0)$. $(1 - Pa_J)$ and P/τ_J^∞ correspond respectively to the amplitude at $t = 0$ and the rate of the decrease of the Markovian exponential at long delays. The relaxation time τ_J^∞ is directly related to the pressure-normalized Lorentz width of the line J. The second term of this equation describes the non-Markovian behavior at times close to $t = 0$. Figures 10a,b show the computed $\rho_J(t)/\rho_J(t=0)$ and their fits with Eq. (1) for $J = 1$ and $J = 8$ as well as the fits using a single exponential decay [i.e. only the first term of Eq. (1)]. It is clear that the evolution at short time is completely different from that at longer time scales.

The relaxation times τ_J^∞/P and τ_J^0 as well as the magnitude Pa_J in Eq. (1), obtained from fits of the relative population for each value of J are presented in Fig. 11. The amplitude a_J of the short time contribution, within the approximations mentioned above (i.e. no influence of line mixing and no contribution of dephasing collisions), is directly related to the intensity correction parameter ΔS. As can be observed in Fig. 11a, a_J being constant with pressure, Pa_J is indeed proportional to pressure as expected and behaves similarly as ΔS (Fig. 8) with the rotational quantum number. Its values are, however, larger than those deduced from the rCMDS-calculated spectra. The relaxation time constant τ_J^0 (Fig. 11c), associated with the molecules which are interacting with another at time t = 0 is independent of pressure which can be explained by the fact that this relaxation time is directly related to the delays needed for an ongoing collision to be completed. At 1 atm, τ_J^0 is more than two orders of magnitude smaller than τ_J^∞. Longer time scale decays, governed by τ_J^∞/P, involve HCl-HCl pairs which are much further apart at t = 0. Since the mean free path is inversely proportional to the pressure, the average delay needed for a collision to occur and thus the associated time constant τ_J^∞/P is thus inversely proportional to the pressure.

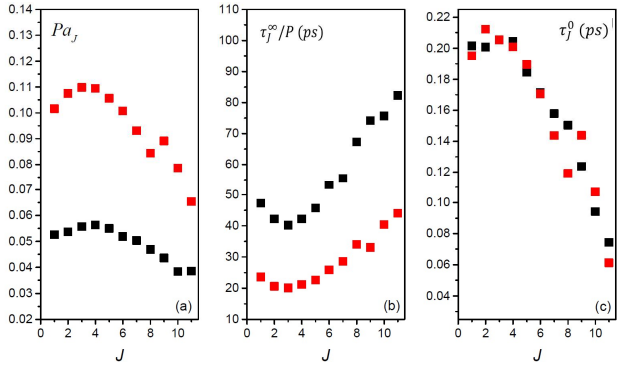

Fig. 11: The magnitude Pa_J and the relaxation time constants τ_J^∞/P and τ_J^0 obtained from fits, using Eq. (1) of the relative populations. The black and red squares are values obtained from calculations at 1 and 2 atm, respectively.

From Eq. (1), and as demonstrated by Fig.10c, the corresponding spectrum includes a narrow and strong Lorentzian peak, of area $(1 - Pa_J)\rho_J(t=0)$ and of HWHM $\Gamma_J^{Lorentz} = P/(2\pi c\tau_J^\infty)$. This contribution, associated with the Fourier transform of the first term in Eq. (1), is carried by a much weaker and broader Lorentzian [of HWHM, $\Gamma_J^{super-Lorentz} = 1/(2\pi c\tau_J^0)$ and of area $Pa_J\rho_J(t=0)$], which is directly the Fourier transform of the second term of Eq. (1). This second term explains the super-Lorentzian behavior observed in the troughs between lines. Fitting the total spectrum with a usual Lorentz-wings profile (e.g. Ref. [24] and references therein) will therefore underestimate the line area (and thus the line intensity). Following this model, the ratio of the total spectrum to the Lorentz calculation at the line center is:

$$\alpha/\alpha_{Lorentz} = \frac{\left\{\frac{S(1-Pa_J)}{\Gamma_J^{Lorentz}} + \frac{SPa_J}{\Gamma_J^{super-Lorentz}}\right\}}{\frac{S}{\Gamma_J^{Lorentz}}}$$

$$= 1 - Pa_J + Pa_J\Gamma_J^{Lorentz}/\Gamma_J^{super-Lorentz} \qquad (2)$$

S being the line intensity. Since for pure HCl, a_J is about 0.03 atm^{-1} (see Fig. 8) and in the considered pressure range the ratio $\Gamma_J^{Lorentz}/\Gamma_J^{super-Lorentz}$ is much smaller than 1 ($\Gamma_J^{super-Lorentz}$ being up to two orders of magnitude larger than $\Gamma_J^{Lorentz}/P$), $\alpha/\alpha_{Lorentz}$ is thus smaller than 1 at the line centers, which is consistent with results observed in Figs. 2 and 9. For HCl in Ar [4], since a_J is smaller than 0.01 atm^{-1} and significant for the two first rotational quantum numbers only[6], the ratio $\alpha/\alpha_{Lorentz}$ is there essentially close to unity at the line centers, as shown in Fig. 1 of Tran at al[4]. In the line wings, when $\Gamma_J^{Lorentz}$ is negligible compared to the wavenumber detuning (i.e. $\Gamma_J^{Lorentz} \ll |\Delta\sigma|$), we can deduce that:

$$\frac{\alpha}{\alpha_{Lorentz}} = 1 - Pa_J + \frac{a_J \Gamma_J^{super-Lorentz}}{\left\{\gamma_J^{Lorentz}\left[1 + \left(\Gamma_J^{super-Lorentz}/|\Delta\sigma|\right)^2\right]\right\}} \quad (3)$$

with $\gamma_J^{Lorentz} = \Gamma_J^{Lorentz}/P$. In this equation, the last term is independent of pressure and much larger than the second term in the considered pressure range. The ratio $\alpha/\alpha_{Lorentz}$ in the troughs between lines is therefore larger than 1 and decreases with increasing pressure, which is also consistent with the results plotted in Fig. 2. Recall that, since the line-mixing effect is not taken into account in this model, the latter cannot explain the behavior of $\alpha/\alpha_{Lorentz}$ in the band wings (see Fig. 2)[4] and it is not valid for pressure conditions for which line-mixing effects are significant.

The proposed analyses, although rather simplified, clearly showed that super-Lorentzian effects between HCl lines and the pressure dependence of the experimentally-determined line intensities are due to incomplete collisions (i.e. collisions that are ongoing), which govern the dipole auto-correlation function at very short times. This also shows that for pure HCl as well as for other systems for which non-impact effects are significant, reliable intensity can be directly obtained from fits of measured spectra with a usual "impact" profile at very low pressure only. For pressures for which the effects are not negligible, the retrieved intensity must be divided by a factor $(1 - \Delta SP)$ to be consistent with the "true" line intensity.

5. Conclusions

Using spectra of pure HCl measured in the first overtone band at room temperature and various pressures between 1 and 10 atm, we showed that the line intensities retrieved from fits of the measurements with the Voigt profile revealed large relative decreases, with increasing pressure, of up to 3%/atm. Contrary to what was observed so far for other molecules/systems, this pressure dependence of the line intensity slowly decreases with the rotational quantum number. On the other hand, the absorptions between successive P and R transitions are significantly larger than those predicted using Voigt profiles. Theoretical predictions were made using requantized classical molecular dynamics simulations (rCMDS), based on intermolecular interaction. The rCMDS predictions lead to good agreement with observations. Our analysis shows that these effects are essentially due to incomplete collisions, which govern the dipole auto-correlation function at very short times and that these ongoing collisions transfer intensity from the core region of the line and reduce its area by shifting a fraction of the latter into a broad and weak continuum. Therefore, fitting measured spectra with a standard Lorentzian-wings line shape model will lead to a reduced line area, which will lead to non-negligible errors in the measured line intensities. Non-impact effects therefore should be taken into account in high accuracy measurements of line intensities, especially when experiments are made at relatively high pressure. This is all the more important as ab initio calculations of line intensities now can achieve accuracies at the few 0.1% level, implying that the measurements used to validate them should have a comparable uncertainty. In addition, extremely accurate intensities and spectral shapes are also required in atmospheric applications such as the detection of greenhouses gases sinks and sources from space observations[25,26]. The higher-pressure range was mostly omitted in previous laboratory spectral measurements aiming on studying the terrestrial atmosphere. To meet the ambitious 0.1% accuracy goal for future GHG observational missions, the amplitude of the super-Lorentzian effects should be precisely quantified. Our results also open perspectives for future studies of the limits of the Markov approximation for inter-molecular collision effects on absorption spectra. Finally, for HCl, the influence of the collision-partner on these non-impact effects will be investigated in a forthcoming study.

Author Contributions

Ha Tran: Conceptualization, Methodology, Data curation, Investigation, Software, Writing-Review-Editing, Gang Li: Data curation, Investigation, Writing-Review-Editing, N. H. Ngo; Software, Investigation; Volker Ebert: HCl measurement design, Review-Editing.

Conflicts of interest

There are no conflicts to declare

Acknowledgements

We acknowledge support by M. Gisi in the HCl measurement execution as described in Ref. [11].

References

1 W. S. Benedict, R. Herman, G. M. Moore and S. Silverman. Can. J. Phys., 1956, **34**, 850.
2 P. Varanasi, S. K. Sarangi and G. D. T. Tejwani. J. Quant. Spectrosc. Rad. Transf., 1972, **12**, 857.
3 J. P. Houdeau, C. Boulet and D. Robert. J. Chem. Phys., 1985, **82**, 1661.
4 H. Tran, G. Li, V. Ebert and J.-M. Hartmann. J. Chem. Phys., 2017, **146**, 194305.
5 A. P. Kouzov, K. G. Tokhadze and S. S. Utkina. Eur. Phys. J. D, 2000, **12**, 153.
6 C. Boulet, P.-M. Flaud and J.-M. Hartmann. J. Chem. Phys., 2014, **120**, 11053.
7 M. O. Bulanin, A. V. Domanskaya, K. Kerl and C. Maul. Mol. Phys., 2006, **104**, 2685.
8 A. P. Kouzov, A. V. Sokolov, and N. N. Filippov. J. Quant. Spectrosc. Rad. Transf., 2022, 278, 108043.
9 A. A. Vigasin and S.V. Ivanov. Chem. Phys., 2006, **325**, 404.
10 D. R. Zachary, H. Tran, N. H. Ngo, J.-M. Hartmann and J. T. Hodges. Phys. Rev. Let., 2023, in revision.
11 G. Li, A. Serdyukov, M. Gisi, O. Werhahn and V. Ebert. J. Quant. Spectrosc. Rad. Transf., 2015, **165**, 76.
12 G. Li, A. V. Domanskaya, H. Tran, M. Gisi and V. Ebert. J. Quant. Spectrosc. Rad. Transf., 2017, **203**, 434.
13 A.V. Domanskaya, G. Li, H. Tran, M. Gisi and V. Ebert. J. Quant. Spectrosc. Rad. Transf., 2017, **199**, 71.

14 F. Hase, T. Blumenstock and C. Paton-Walsh. Appl. Opt., 1999, **38**, 3417.
15 F. Hase. Atmos. Meas. Tech., 2012, **5**, 603.
16 P. W. Rosenkranz, IEEE Trans. Antennas Propag., 1975, **23**, 498.
17 I.E. Gordon, L.S. Rothman, R.J. Hargreaves, R. Hashemi, E.V. Karlovets, F.M. Skinner, E.K. Conway, C. Hill, R.V. Kochanov, Y. Tan, P. Wcisło, A.A. Finenko, K. Nelson, P.F. Bernath, M. Birk, V. Boudon, A. Campargue, K.V. Chance, et al. J. Quant. Spectrosc. Rad. Transf., 2022, **277**, 107949.
18 P. K. Naicker, A. K. Sum and S. I. Sandlera. J. Chem. Phys., 2003, **118**, 4086.
19 A. S. Pine and A. Fried. J. Mol. Spectrosc., 1985, **114**, 148.
20 L.S. Rothman, I.E. Gordon,Y. Babikov, A. Barbe, D. C. Benner, P.F. Bernath, M. Birk, L. Bizzocchi, V. Boudon, L. R. Brown, A. Campargue, K. Chance, E. A. Cohen, L. H. Coudert et al. J. Quant. Spectrosc. Rad. Transf., 2013, **130**, 4.
21 H. Tran and J.-L. Domenech. J. Chem. Phys., 2014, **141**, 064313.
22 M. P. Allen and D. J. Tildesley, *Computer simulations of liquids* (Oxford, Oxford University Press, 1987).
23 J.-M. Hartmann, C. Boulet, and D. Robert, *Collisional Effects on Molecular Spectra. Laboratory Experiments and Models, Consequences for Applications* (Elsevier, Amsterdam, 2008).
24 N. H. Ngo, D. Lisak, H. Tran and J.-M. Hartmann. J. Quant. Spectrosc. Rad. Transf., 2013, **129**, 89.
25 C. E. Miller, L. R. Brown, R. A. Toth, D. C. Benner and V. M. Devi. C. R. Physique, 2005, **6**, 876.
26 T. Delahaye, S. E. Maxwell, Z. D. Reed, H. Lin, J. T.Hodges, K. Sung, V. M. Devi, T.Warneke, P. Spietz and H. Tran. J. Geophys. Res., 2016, **121**, 7360.